REPORT

Bi-allelic *CCDC47* Variants Cause a Disorder Characterized by Woolly Hair, Liver Dysfunction, Dysmorphic Features, and Global Developmental Delay

Marie Morimoto,[1,15] Helen Waller-Evans,[2,15] Zineb Ammous,[3,15] Xiaofei Song,[4,15] Kevin A. Strauss,[5] Davut Pehlivan,[4] Claudia Gonzaga-Jauregui,[6] Erik G. Puffenberger,[5] Charles R. Holst,[7] Ender Karaca,[4] Karlla W. Brigatti,[5] Emily Maguire,[2] Zeynep H. Coban-Akdemir,[4] Akiko Amagata,[7] C. Christopher Lau,[1] Xenia Chepa-Lotrea,[1] Ellen Macnamara,[1] Tulay Tos,[8] Sedat Isikay,[9] Michele Nehrebecky,[1] John D. Overton,[6] Matthew Klein,[7] Thomas C. Markello,[1] Jennifer E. Posey,[4] David R. Adams,[1,10,11] Emyr Lloyd-Evans,[2] James R. Lupski,[4,12,13,14] William A. Gahl,[1,10,11] and May Christine V. Malicdan[1,10,11,*]

Ca^{2+} signaling is vital for various cellular processes including synaptic vesicle exocytosis, muscle contraction, regulation of secretion, gene transcription, and cellular proliferation. The endoplasmic reticulum (ER) is the largest intracellular Ca^{2+} store, and dysregulation of ER Ca^{2+} signaling and homeostasis contributes to the pathogenesis of various complex disorders and Mendelian disease traits. We describe four unrelated individuals with a complex multisystem disorder characterized by woolly hair, liver dysfunction, pruritus, dysmorphic features, hypotonia, and global developmental delay. Through whole-exome sequencing and family-based genomics, we identified bi-allelic variants in *CCDC47* that encodes the Ca^{2+}-binding ER transmembrane protein CCDC47. CCDC47, also known as calumin, has been shown to bind Ca^{2+} with low affinity and high capacity. In mice, loss of *Ccdc47* leads to embryonic lethality, suggesting that Ccdc47 is essential for early development. Characterization of cells from individuals with predicted likely damaging alleles showed decreased *CCDC47* mRNA expression and protein levels. *In vitro* cellular experiments showed decreased total ER Ca^{2+} storage, impaired Ca^{2+} signaling mediated by the IP_3R Ca^{2+} release channel, and reduced ER Ca^{2+} refilling via store-operated Ca^{2+} entry. These results, together with the previously described role of CCDC47 in Ca^{2+} signaling and development, suggest that bi-allelic loss-of-function variants in *CCDC47* underlie the pathogenesis of this multisystem disorder.

Ca^{2+} signaling is a multipurpose intracellular signaling system that regulates a number of cellular processes including synaptic vesicle exocytosis, muscle contraction, regulation of secretion, transcription, and cellular proliferation.[1] The endoplasmic reticulum (ER), or the sarcoplasmic reticulum (SR) in muscle cells, is the largest store of intracellular Ca^{2+}.[2] ER Ca^{2+} depletion is also observed in a number of genetic disorders due to variants in Ca^{2+} channels and sensors. For example, Brody myopathy (MIM: 601003) is caused by recessive variants in *ATP2A1* (MIM: 611974), which encodes the fast-twitch skeletal muscle sarcoplasmic reticulum Ca^{2+} ATPase (SERCA1),[3] while Darier disease (MIM: 124200) occurs due to variants in *ATP2A2* (MIM: 108740), which encodes another sarcoplasmic reticulum Ca^{2+} ATPase, SERCA2.[4] Minicore myopathy (MIM: 255320) and central core disease (MIM: 117000) result from variants in *RYR1* (MIM: 180901), which encodes a major Ca^{2+} release channel,[5] and autosomal centronuclear myopathy (MIM: 160150) is associated with variants in *MTMR14* (MIM: 611089), which encodes a muscle-specific inositol phosphatase.[6] Stormorken syndrome (MIM: 185070), tubular aggregate myopathy 1 (MIM: 160565), and immunodeficiency 10 (MIM: 612783) are caused by variants in *STIM1* (MIM: 605921),[7–9] which encodes a Ca^{2+} sensor. Tubular aggregate myopathy 2 (MIM: 615883) and immunodeficiency 9 (MIM: 612782) are caused by variants in *ORAI1* (MIM: 610277),[10,11] which encodes a Ca^{2+} channel that coordinates ER Ca^{2+} refilling via store-operated Ca^{2+} entry (SOCE). Additionally, disruption of ER Ca^{2+} homeostasis contributes to the pathogenesis of several common diseases including diabetes mellitus, neurological diseases, and cancer.[12]

CCDC47, also known as calumin, is present in several tissues including brain, lung, heart, stomach, liver, spleen, kidney, muscle, and testis.[13] CCDC47 is an ER transmembrane Ca^{2+}-binding protein involved in embryogenesis and development.[13,14] A reported *Ccdc47*-knockout mouse model exhibited delayed development, atrophic neural

[1]National Institutes of Health Undiagnosed Diseases Program, Common Fund, Office of the Director, National Institutes of Health, Bethesda, MD 20892, USA; [2]School of Biosciences, Cardiff University, Cardiff CF10 3AX, UK; [3]The Community Health Clinic, Topeka, IN 46571, USA; [4]Department of Molecular and Human Genetics, Baylor College of Medicine, Houston, TX 77030, USA; [5]Clinic for Special Children, Strasburg, PA 17579, USA; [6]Regeneron Genetics Center, Regeneron Pharmaceuticals Inc., Tarrytown, NY 10591, USA; [7]BioElectron Technology Corporation, Mountain View, CA 94043, USA; [8]Department of Medical Genetics, Dr. Sami Ulus Research and Training Hospital of Women's and Children's Health and Diseases, Ankara 06080, Turkey; [9]Department of Physiotherapy and Rehabilitation, Hasan Kalyoncu University, School of Health Sciences, Gaziantep 27000, Turkey; [10]Medical Genetics Branch, National Human Genome Research Institute, National Institutes of Health, Bethesda, MD 20892, USA; [11]Office of the Clinical Director, National Human Genome Research Institute, National Institutes of Health, Bethesda, MD 20892, USA; [12]Department of Pediatrics, Baylor College of Medicine, Houston, TX 77030, USA; [13]Human Genome Sequencing Center, Baylor College of Medicine, Houston, TX 77030, USA; [14]Texas Children's Hospital, Houston, TX 77030, USA
[15]These authors contributed equally to this work
*Correspondence: maychristine.malicdan@nih.gov
https://doi.org/10.1016/j.ajhg.2018.09.014.

Table 1. Summary of Clinical Features of Individuals with Bi-allelic Loss-of-Function *CCDC47* Variants

Clinical Features	Proband 1	Proband 2	Proband 3	Proband 4
Prenatal and Perinatal History				
Delivery	C-section	C-section	NSVD	C-section
Premature birth	+	term	term	term
Polyhydramnios	+	–	–	–
Respiratory distress	–	NA	+	+
Decreased fetal movements	NA	+	+	NA
Bradycardia	+	+	–	+
Birth weight (%ile)	75th	NA	<3rd	10th
Growth Parameters				
Decreased body weight	+	+	+	+
Microcephaly	+	+	+	+
Physical Findings				
Coarse facies	+	+	+	+
Midface hypoplasia	+	+	+	–
Hypertelorism	+	+	+	–
Almond-shaped palpebral fissure	+	+	–	–
Epicanthal folds	–	–	+	–
Ptosis	+	+	+	+
Long eyelashes	+	+	–	–
Synophrys	+	–	+	+
Ectropion	+	+	–	–
Unusual nose	+	+	+	+
Downturned mouth	+	+	+	+
Macrostomia	–	+	wide mouth	–
Macroglossia	–	+	+	+
Full or thick lips	+	+	+	+
Dental abnormalities	+	–	+	+
High arched palate	+	+	+	+
Ear abnormalities	+	+	+	+
Bilateral otitis media	+	+	+	+
Bitemporal narrowing	–	+	+	+
Brachycephaly	+	+	+	+
Plagiocephaly	+	+	+	–
Pruritus	+	+	+	+
Unusual hair	+	+	+	+
Thoracic hypertrichosis	+	+	+	+
Fifth digit hypoplasia and/or clinodactyly	+	+	+	+
Dystrophic nails	–	–	+	–
Overlapping toes	+	+	+	+
Distal arthrogryposis / joint laxity	+	+	+	+
Hypoplastic nipples	+	+	+	+

(*Continued on next page*)

Table 1. ***Continued***

Clinical Features	Proband 1	Proband 2	Proband 3	Proband 4
Genital anomaly	+	+	–	–
Musculoskeletal Findings				
Hypotonia	+	+	+	+
Bilateral hip dislocation	+	+	ND	–
Hip dysplasia	+	+	ND	+
Bilateral coxa valga	+	–	ND	+
Abnormal bone density	+	+	ND	ND
Narrow chest	+	+	–	–
Fibular bowing	+	+	–	–
Genu valgum	–	–	+	–
Bilateral clubfoot	+	+	–	+
Small feet	+	+	+	+
Pectus excavatum	+	–	–	+
Scoliosis	–	+	+	–
Ocular Findings				
Hyperopia	+	NA	–	+
Astigmatism	+	NA	–	–
Cortical visual impairment	+	NA	+	+
Immunological Findings				
Recurrent infections	–	+	+	–
Immunodeficiency	–	+	+	–
Endocrine Findings				
Hypothyroidism	–	NA	+	–
Rickets	–	+	+	–
Respiratory Findings				
Obstructive sleep apnea	+	+	+	–
Central sleep apnea	+	NA	+	–
Heart Findings				
Ventricular septal defect	–	+	–	–
Patent ductus arteriosus	+	+	–	–
Gastrointestinal Findings				
Hepatosplenomegaly	+	–	+	–
Liver dysfunction	+	ND	+	+
Recurrent pancreatitis	+	NA	–	–
Exocrine pancreatic insufficiency	+	NA	–	–
Gastresophageal reflux	+	NA	+	+
Steatorrhea	+	+	–	–
Chronic diarrhea	–	+	–	+
Gallstones	+	–	–	+
Gastrostomy tube	+	–	+	+

(*Continued on next page*)

Table 1. ***Continued***

Clinical Features	Proband 1	Proband 2	Proband 3	Proband 4
Elevated bile acids	+	NA	+	+
Renal Findings				
Renal abnormalities	+	+	–	–
Neurological Findings				
Severe global developmental delay	+	+	+	+
Hyperreflexia	–	–	+	+
Reduced tendon reflexes	+	+	–	–
Absent Achilles reflex	+	+	–	–
Behavioral issues	–	–	+	+
Seizures	–	NA	+	–
EEG abnormalities	+	NA	+	+
Neuroimaging Findings				
Abnormal ventricle morphology	+	+	–	+
Abnormal corpus callosum	+	–	–	+
Cerebral atrophy	+	+	+	+
White matter abnormalities	–	–	–	+
Cerebellar hypoplasia	–	–	–	+

Abbreviations: +, present; – absent; C-section, Caesarean section; EEG, electroencephalogram; NA, not available; ND, not done; NSVD, normal spontaneous vaginal delivery.

tubes, heart abnormalities, a paucity of blood cells in the dorsal aorta, and embryonic lethality.[14] Further, mouse embryonic fibroblasts (MEFs) from these mice exhibited impaired Ca^{2+} signaling.[13] These data suggest that CCDC47 is critical for Ca^{2+} signaling and normal development.

In this study, we report four unrelated individuals presenting with a complex multisystem disorder characterized by woolly hair, liver dysfunction, pruritus, dysmorphic features, hypotonia, and global developmental delay; the clinical features of the probands are summarized in Table 1. We performed molecular analyses on probands who were referred to one of the collaborating centers for diagnostic evaluation of an undiagnosed genetic disorder and for whom prior genetic testing had been unrevealing. The parents of probands 1, 3, and 4 provided informed consent for sample collection and molecular analyses under protocol 76-HG-0238 approved by the NHGRI Institutional Review Board. The family of proband 2 gave consent for research studies through the Baylor-Hopkins Center for Mendelian Genomics (BHCMG) initiative under protocol #H-29697 approved by the Institutional Review Board at Baylor College of Medicine. The families of probands 3 and 4 were recruited for research studies through the Clinic for Special Children under a Lancaster General Hospital Institutional Review Board-approved protocol. Blood samples were collected from the probands and their unaffected parents and, when available, their unaffected siblings for whole-exome sequencing. Skin biopsies or peripheral blood leukocytes were obtained from the proband when possible for further molecular analyses. Using whole-exome sequencing, we identified bi-allelic variants in *CCDC47* that encodes the Ca^{2+}-binding ER transmembrane protein CCDC47. Further details on the methodologies used in this study are available in the Supplemental Data.

Proband 1 (1: II-1) was a 5-year-old female at the time she was evaluated through the National Institutes of Health Undiagnosed Diseases Program.[15–17] She was born to non-consanguineous parents of mixed Northern European and Native American descent. There were three miscarriages subsequent to the birth of proband 1. The pregnancy was complicated by premature rupture of membranes at 30 weeks of gestation, requiring preterm delivery by Caesarean section. At birth, she exhibited microcephaly, hypotonia, bilateral club foot deformities, and a patent ductus arteriosus (PDA). Complete blood counts identified anemia during infancy, which resolved by 5 years of age. She was unable to breast or bottle feed and was admitted to the NICU, where she was diagnosed with oral motor dyspraxia and severe gastresophageal reflux (GERD). At approximately 3 years of age, she experienced an episode of pancreatitis with liver inflammation. She had recurrent steatorrhea and low fecal elastase levels, and multiple gray-black cholesterol stones; cholecystectomy failed to resolve the problem and she underwent recurrent hospitalizations for similar episodes of pancreatitis. Evaluations for primary biliary cholangitis and autoimmune hepatitis were negative, and she was diagnosed with exocrine pancreatic

insufficiency. She had dysmorphic facial features including coarse and woolly hair, midface hypoplasia, hypertelorism, ptosis, a downturned mouth, full lips, dental abnormalities, a high arched palate, low-set ears, brachycephaly, and plagiocephaly (Figure 1A and Table 1). Further clinical examination revealed distal arthrogryposis, fifth digit hypoplasia, a narrow chest, hypoplastic nipples, hip dysplasia, clitoral hyperplasia, fibular bowing, and overlapping toes (Figure 1A and Table 1). Ophthalmologic evaluation showed astigmatism, hyperopia, and cortical visual impairment. Skeletal survey was consistent with osteopenia. She exhibited both truncal and appendicular hypotonia with poor head control and severe global developmental delay. She had frog leg posturing when supine. She could not hold objects, bear weight, or sit up without support. A brain MRI showed abnormalities of the corpus callosum as well as mild prominence of the third ventricle (Figure S1A). Additional clinical data are available in the Supplemental Note.

Proband 2 (2: II-3) was a male first seen by the Department of Medical Genetics at Dr. Sami Ulus Research and Training Hospital of Women's and Children's Health and Diseases at age 2 years 7 months. He was born at term via Caesarean section with a birth weight of 3,000 g. The parents were first-degree cousins of Turkish origin and they had two healthy living children and reported four previous miscarriages as well as two miscarriages subsequent to the birth of proband 2. The parents first noticed decreased spontaneous movements and hypotonia at 2 months of life. The infant had no head control and no single words. He was below the 3rd percentile for all anthropometric measurements, with severe malnutrition. Dysmorphic features included woolly and thin blonde hair, macroglossia, macrostomia, and simple large ears (Figure 1B and Table 1). The proband also exhibited bilateral cryptorchidism. Ophthalmologic evaluation was unremarkable. Laboratory studies including chemistry, blood count, metabolic testing (urine organic acid, ammonia, plasma amino acid, lactate, and pyruvate), congenital disorders of glycosylation testing, karyotype, and subtelomeric FISH were negative or inconclusive. Echocardiogram showed a ventricular septal defect (VSD) and PDA; abdominal ultrasound revealed nephrocalcinosis. Skeletal survey was consistent with osteoporosis (Figure S1B). Brain CT showed mild dilation of the lateral ventricles and cerebral atrophy. The boy was last evaluated at age 8 and the mother had two more miscarriages in the interim. He was referred to Baylor-Hopkins Center for Mendelian Genomics (BHCMG) to identify the molecular etiology.

Proband 3 (3: II-8) was an Old Order Amish female first seen at The Community Health Clinic (Topeka, IN) at age 7 years 7 months. She was born at 38 weeks of gestation via normal spontaneous vaginal delivery at home with a birth weight of 2,070 g and considered to be small for gestational age. The mother noticed slower and less frequent movements compared to her previous pregnancies. Due to respiratory distress, the newborn was transported to Wright Memorial Hospital (Trenton, MO) where she was placed on oxygen for 12–24 hr. She was frequently ill and diagnosed with failure to thrive (FTT); at 3 months of age a gastrostomy tube (G-tube) was placed. Dysmorphic features included microcephaly, dark and curly hair, epicanthal folds, hypertelorism, a bulbous nasal tip, and a wide and downturned mouth (Figure 1C and Table 1). She also had small hands and feet, dystrophic nails, and abnormal chubby toes that overlapped (Figure 1C and Table 1). The proband had a history of feeding issues, FTT, GERD, and liver dysfunction with mild splenomegaly and a prominent left hepatic lobe; itching improved on cholestyramine. She had recurrent infections due to a Toll-like receptor signaling defect, which was treated with IVIG, as well as central hypothyroidism and vitamin D-deficient rickets. Proband 3 also had chronic respiratory insufficiency and a history of apnea and sleep disturbances. Developmentally, she was severely delayed, nonverbal, and had generalized hypotonia. She could not grasp objects or sit up but was able to roll onto her side. Behaviorally, she displayed bruxism and self-mutilation; treatment with Risperdal resolved these behaviors. A brain MRI revealed mild prominence of the CSF space (Figure S1A). The parents had five healthy living children, two miscarriages, and two males who passed away at 3.5 months (3: II-3) due to aspiration pneumonia and at 7 months of gestation (3: II-6) (Figure 2A). A maternal uncle passed away at 9 weeks of age due to kidney failure. All had dark curly hair similar to proband 3 (3: II-8). Additional clinical data are available in the Supplemental Note.

Proband 4 (4: II-1) was first seen at The Community Health Clinic (Topeka, IN) at age 6 years 6 months. At birth, she was transferred to the Memorial Hospital NICU (South Bend, IN) for 5 days due to episodes of oxygen desaturation and poor feeding. At 1 year 6 months, she had a G-tube placed due to FTT. Her dysmorphic features included microcephaly, red curly hair, synophrys, full lips, and a downturned mouth (Figure 1D and Table 1). A skeletal survey showed that she had bilateral talipes equinovarus, coxa valga, bilateral overlapping toes, pectus excavatum, and hypermobile joints (Figure 1D and Table 1). Ophthalmologic evaluation showed she had hyperopia and cortical visual impairment. Proband 4 had abnormal liver function tests, elevated serum bile acids, and pruritus; itching improved on cholestyramine. She also had cholelithiasis without secondary evidence of acute cholecystitis; partial visualization of the pancreas was unremarkable. Neurologically, she had severe global developmental delay, hyperreflexia, hypotonia, and poor head control; she was non-verbal, although she sometimes answered "yah." She displayed bruxism and self-mutilation and also clapped or hit herself when excited. A brain MRI showed minimal prominence of the cerebral sulci and ventricular enlargement, global white matter paucity, and a thin corpus callosum (Figure S1A). The parents had three healthy living children subsequent to the birth of

Figure 1. Clinical Physical Features of the Four Probands with Bi-allelic Loss-of-Function *CCDC47* Variants
All four probands have dysmorphic facial features characterized by coarse facies, ptosis, a downturned mouth, simple ears, and unusual hair that is coarse and/or woolly and/or curly. Microcephaly, brachycephaly, hypotonia, joint laxity/distal arthrogryposis, nipple hypoplasia, and overlapping toes were also present in all of the probands. Other dysmorphic features observed in most of the probands include midface hypoplasia, hypertelorism, dental abnormalities, plagiocephaly, a narrow chest, hip dysplasia, and bilateral clubfoot.

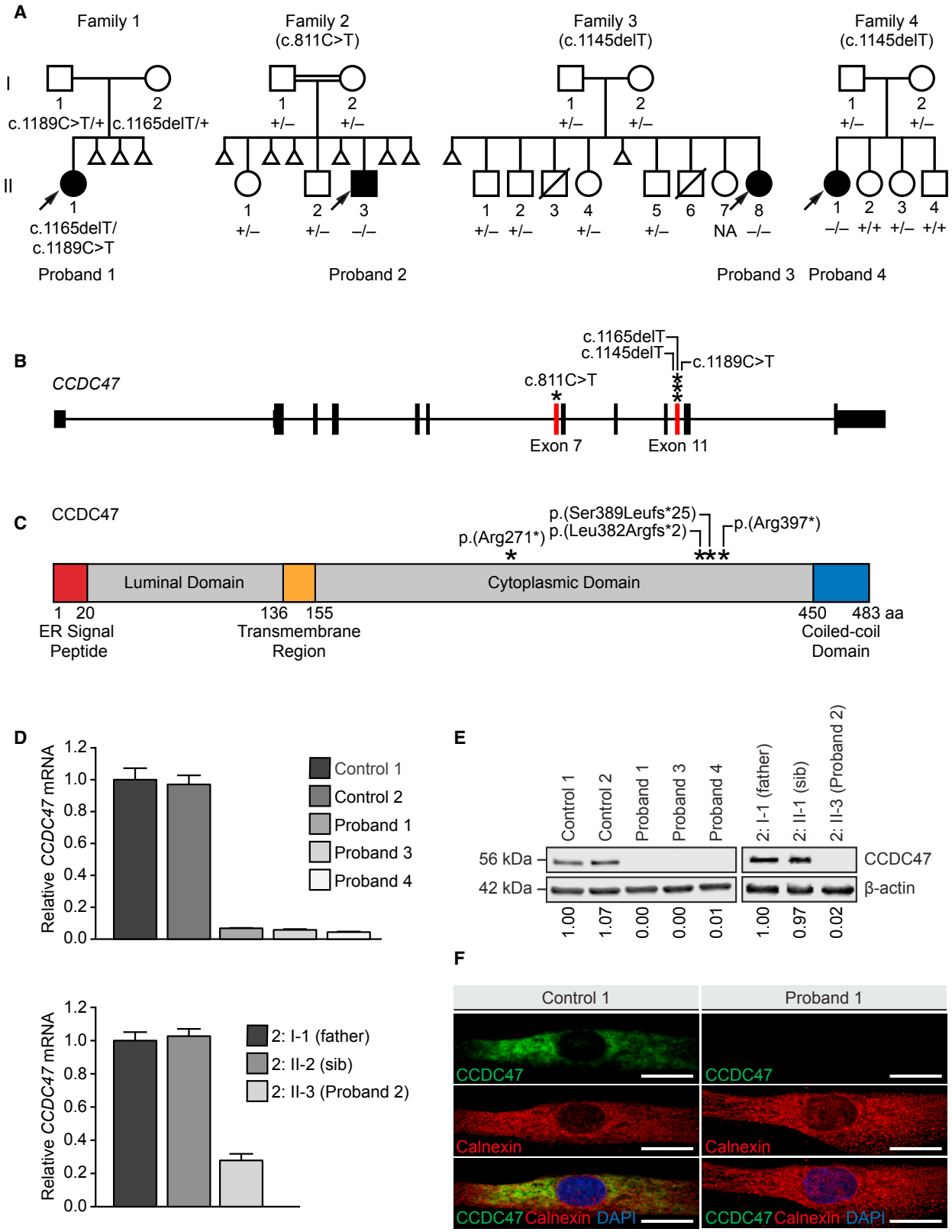

Figure 2. Bi-allelic *CCDC47* Variants Segregate with Disease in All Four Families and Lead to Decreased *CCDC47* mRNA Expression and CCDC47 Protein Levels

(A) The pedigrees of all four families with a proband exhibiting woolly hair, liver dysfunction, pruritus, dysmorphic features, and developmental delay show segregation of *CCDC47* (GenBank: NM_020198.2) variants in an autosomal-recessive mode of inheritance. Note recurrent pregnancy loss in three of four pedigrees.

(B) Schematic of *CCDC47* showing the locations of the variants (asterisks) leading to a frameshift or stop-gain variant in exon 7 and 11 (red bars).

(legend continued on next page)

the proband (Figure 2A). Additional clinical data are available in the Supplemental Note.

Whole-exome sequencing was performed on these four probands at three different research centers to identify pathogenic variants underlying their disease (Supplemental Subjects and Methods).[18] Variant interpretation and prioritization was based on the clinical relevance of the gene and the pathogenicity of the variants using ACMG-AMP guidelines.[19] Further variant prioritization was based on Mendelian consistency and segregation, observed frequency of the variants in public and internal population databases, conservation, and predicted deleteriousness coalesced with published biological and functional data of the candidate genes. Each center independently identified compound heterozygous or homozygous variants in *CCDC47* (GenBank: NM_020198.2) segregating according to Mendelian expectations for an autosomal-recessive disease trait (Figures 2A, 2B, and S2; Table 2). All of the *CCDC47* variants identified were either nonsense or frameshift variants that are predicted to lead to nonsense-mediated mRNA decay or premature truncation of the protein (Figure 2C and Table 2). The allele frequencies of the identified *CCDC47* variants in population databases, such as the Genome Aggregation Database (gnomAD), were very low ranging from 0.000% to 0.010% (Table 2) with no homozygotes recorded. In addition, these variants are predicted to be pathogenic by multiple bioinformatic algorithms (Table 2).

To experimentally assess the functional consequences of the variants identified, we performed TaqMan gene expression analysis to quantify *CCDC47* mRNA, western blot to assess the levels of CCDC47, and indirect immunofluorescence microscopy to assess the localization of the protein (Supplemental Subjects and Methods and Tables S1–S3). Gene expression analyses showed that the relative *CCDC47* mRNA was decreased in the primary dermal fibroblasts of probands 1 (1: II-1), 3 (3: II-8), and 4 (4: II-1) compared to two unaffected sex-matched pediatric controls (Figure 2D, upper panel) and in the lymphoblastoid cells of proband 2 (2: II-3) compared to his father (2: I-1) and unaffected sibling (2: II-2) (Figure 2D, lower panel). Consistent with the predicted loss-of-function effect of the identified variants, CCDC47 levels were nearly undetectable in the cells from all four probands, as assessed using an antibody that recognizes the C terminus of CCDC47 (Figure 2E). These results were consistent using an antibody that recognizes the N terminus of CCDC47 (data not shown). Cell studies showed that CCDC47 was localized in an ER-like pattern in unaffected control cells and that the signal for CCDC47 was undetectable by immunofluorescence using primary dermal fibroblasts from proband 1 (Figure 2F), consistent with the observation from western blot experiments. Altogether, our experiments support the hypothesis that the variants in *CCDC47* lead to nonsense-mediated decay of the prematurely truncated transcripts and result in the absence of protein and a functional loss of CCDC47.

To further explore the functional effects of loss of CCDC47, we performed *in vitro* experiments to interrogate ER Ca^{2+} storage, Ca^{2+} release, and store-operated Ca^{2+} entry (SOCE). CCDC47 has been previously shown to bind Ca^{2+},[13] so we hypothesized that the loss of CCDC47 expression would lead to impaired ER Ca^{2+} storage, signaling, and refilling. We performed live-cell imaging using the cell-permeable Ca^{2+} indicator Fura-2-acetoxymethyl ester (Fura-2AM) to monitor the elevation of cytoplasmic Ca^{2+} following the addition of either the sarco/endoplasmic reticulum Ca^{2+}-ATPase (SERCA) inhibitor thapsigargin at a high concentration to completely deplete ER Ca^{2+} levels and assess total ER Ca^{2+}. In addition, IP_3 was used to induce Ca^{2+} release via the inositol 1,4,5-trisphosphate receptor (IP_3R), ryanodine to induce Ca^{2+} release via the ryanodine receptor (RyR), thapsigargin at a low concentration to determine ER Ca^{2+} leak, and thapsigargin at a high concentration to deplete ER Ca^{2+} levels followed by $CaCl_2$ to assess refilling via SOCE (Supplemental Subjects and Methods). Complete inhibition of SERCA, which transports Ca^{2+} from the cytoplasm into the ER, was achieved by the addition of 2 μM thapsigargin, which leads to rapid depletion of ER Ca^{2+} stores and reflects total ER Ca^{2+} levels.[20] Our results show that total ER Ca^{2+} was decreased in the primary dermal fibroblasts of all three probands tested compared to unaffected control cells (Figure 3A). Ca^{2+} release via IP_3R was decreased in the primary dermal fibroblasts of all three probands tested (Figure 3B), while Ca^{2+} release via RyR was decreased only in proband 1 compared to that of unaffected control

(C) Schematic of CCDC47, also known as calumin, and its functional domains showing the locations of the predicted amino acid changes (asterisks).
(D) Relative *CCDC47* mRNA expression was quantified by TaqMan assay in the fibroblast cells of two unaffected control subjects and probands 1, 3, and 4 (upper panel) and in the lymphoblastoid cells of the father (2: I-1) and unaffected sibling (2: II-2) of proband 2 and proband 2 himself (2: II-3, lower panel). Data are presented as the mean of four technical replicates relative to control 1 (upper panel) or the father of proband 2 (2: I-1, lower panel). Expression of *HPRT1* and *POLR2A* were used as internal controls to normalize gene expression; error bars represent one standard deviation.
(E) CCDC47 levels were quantified by western blot using an antibody against the C terminus of CCDC47 in the fibroblasts of two unaffected control subjects and probands 1, 3, and 4 (left panel) and in the lymphoblastoid cells of the father (2: I-1) and unaffected sibling (2: II-2) of proband 2 and proband 2 himself (2: II-3, right panel). Samples were quantified relative to control 1 (left panel) or the father of proband 2 (2: I-1) (right panel). Expression of β-actin levels were used as a loading control to normalize CCDC47 levels.
(F) CCDC47 localization (green) was assessed by indirect immunofluorescence microscopy in the fibroblasts of an unaffected control and proband 1. An antibody against calnexin (red) was used as an ER marker; DAPI (blue) was used to stain the nucleus.
Scale bar = 20 microns. Abbreviations: aa, amino acid; DAPI, 4′,6-diamidino-2-phenylindole; ER, endoplasmic reticulum; NA, not available.

Table 2. Summary of Bi-allelic Loss-of-Function Variants Identified in *CCDC47* (GenBank: NM_020198.2)

Proband	Ancestry	Reported Consanguinity	Nucleotide Change (hg19 genomic coordinates)	Coding Sequence Change	Amino Acid Change	Inheritance	Parent of Origin	gnomAD All	CADD Phred Score	AOH Region Containing Candidate (Mb)	Genomewide AOH (Mb)
1	Northern European/Native American	no	Chr17:g.61829694G>A	c.1189C>T	p.Arg397*	compound heterozygous	P	0.010%	40	NA	NA
			Chr17:g.61829718del	c.1165delT	p.Ser389Leufs*25		M	0.000%	34	NA	NA
2	Turkish	yes	Chr17:g.61833855G>A	c.811C>T	p.Arg271*	homozygous	both	0.001%	39	1.3	268.4
3	Amish	no	Chr17:g.61829738del	c.1145delT	p.Leu382Argfs*2	homozygous	both	0.002%	35	19.6	81.2
4	Amish	no	Chr17:g.61829738del	c.1145delT	p.Leu382Argfs*2	homozygous	both	0.002%	35	15.7	65.1

Abbreviations: AOH, absence of heterozygosity; CADD, Combined Annotation Dependent Depletion; gnomAD, Genome Aggregation Database; M, maternal; NA, not applicable; P, paternal.

subjects (Figure 3C). Although proband 4 has generally lower Ca^{2+} released after addition of ryanodine, the difference from control subjects was not statistically significant. Partial inhibition of SERCA by the addition of 0.2 μM thapsigargin unmasks ER Ca^{2+} leak, a constitutive process mediated via ion channels such as presenilin 1 and bax inhibitor 1.[21,22] ER Ca^{2+} leak was decreased in probands 1 and 4 compared to that of unaffected control subjects (Figure 3D). SOCE was decreased in all three probands tested (Figure 3E), which may indicate inefficient refilling of the ER store via Ca^{2+} entry across the plasma membrane. Overexpression of *CCDC47* in the primary dermal fibroblasts of proband 1 rescued ER Ca^{2+} storage, signaling, and refilling via SOCE (Figures 3 and S3). Together, these Ca^{2+} imaging studies demonstrated that ER Ca^{2+} stores are decreased, ER Ca^{2+} signaling is impaired, and ER Ca^{2+} refilling via SOCE is reduced in the cells of individuals with *CCDC47* variants, suggesting that CCDC47 is important for the maintenance of Ca^{2+} homeostasis and signaling in the ER.

In addition to acting as the largest intracellular Ca^{2+} store, the ER is a dynamic organelle that is involved in protein synthesis, folding, quality control, and secretion. Accumulation of unfolded proteins leads to ER stress and the activation of several signal transduction pathways collectively known as the unfolded protein response (UPR). Three key UPR pathways, including the IRE1α, ATF6, and PERK pathways, have been identified (Figure S4A).[23–26] ER stress leads to IRE1α phosphorylation and subsequent splicing of *XBP1*, which is translated into a transcription factor that translocates into the nucleus (Figure S4A, left panel); and/or the cleavage of ATF6 into a transcription factor that translocates into the nucleus (Figure S4A, center panel); and/or the phosphorylation of PERK and eIF2α that lead to the activation of ATF4, a transcription factor that translocates into the nucleus (Figure S4A, right panel) to induce the transcription of UPR target genes.[23–26] Similar to the observations reported in *Ccdc47*-knockout mouse embryonic fibroblasts (MEFs),[13] primary dermal fibroblasts derived from proband 1 exhibited normal activation of each of the three arms of the UPR upon ER stress with the SERCA inhibitor thapsigargin (Figures S4B–S4D), suggesting that the UPR is functional in these cells.

Ca^{2+} release from the ER to the mitochondria is critical for Ca^{2+}-dependent mitochondrial membrane protein function, mitochondrial division, and apoptosis activation.[27] Further, there is extensive cross talk between Ca^{2+} and reactive oxygen species (ROS) signaling systems, and dysfunction in either system might detrimentally affect the other system.[28] Since Ca^{2+} storage is reduced and signaling is impaired in the ER of fibroblasts from individuals with *CCDC47* variants, we postulated that they may be more susceptible to oxidative stress. To test this, we performed an oxidative stress assay (Supplemental Subjects and Methods). Compared to unaffected control dermal fibroblasts, primary dermal fibroblasts from proband 1

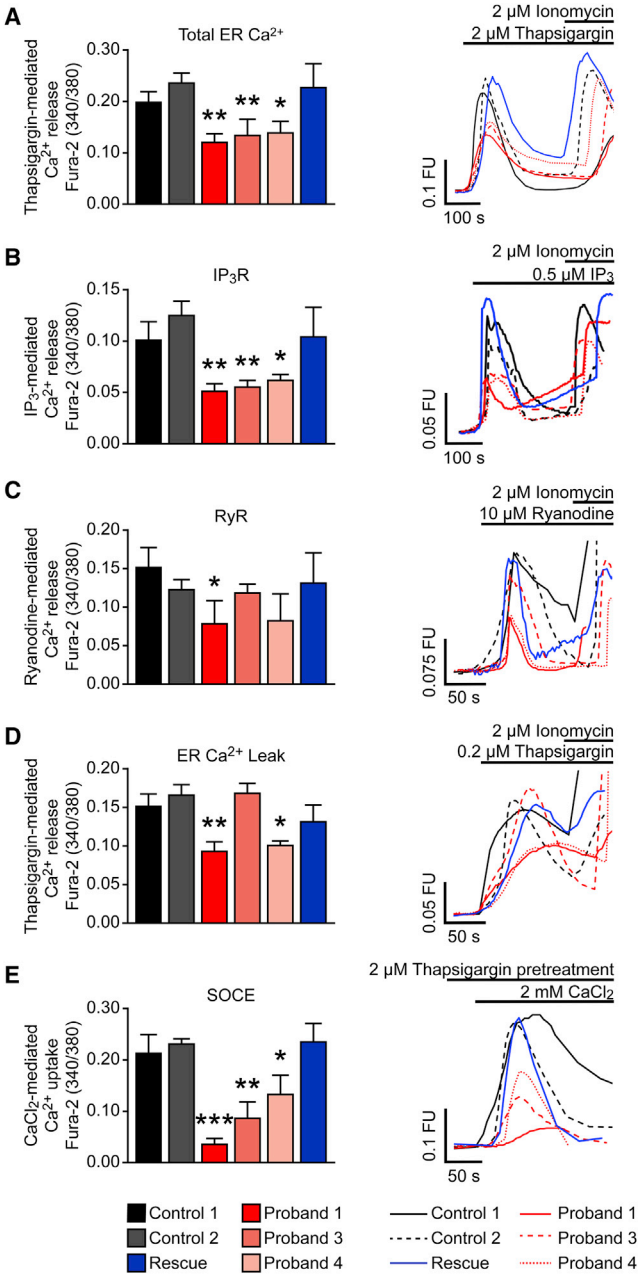

Figure 3. Total ER Ca^{2+} Storage, ER Ca^{2+} Signaling, and ER Ca^{2+} Refilling via Store-Operated Ca^{2+} Entry (SOCE) Are Impaired in Fibroblasts from Individuals with Loss-of-Function Variants in *CCDC47*

Unaffected control fibroblasts (control 1 and control 2), proband 1, 3, and 4 fibroblasts, and a rescue cell line where wild-type *CCDC47* was stably expressed in the dermal fibroblasts from proband 1 (Rescue) were stained and imaged live with the cytosolic Ca^{2+} probe Fura-2AM prior to the addition of 2 μM thapsigargin (A), 0.5 μM IP_3-AM (B), 10 μM ryanodine (C), 0.2 μM thapsigargin (D), or 2 mM $CaCl_2$ following 2 μM thapsigargin pretreatment (E) to measure the release of total Ca^{2+} from the ER, Ca^{2+} release from the ER via the inositol 1,4,5-triphosphate receptor (IP_3R), Ca^{2+} release from the ER via the ryanodine receptor (RyR), Ca^{2+} leak from the ER, or uptake of Ca^{2+} into the ER via SOCE, respectively. The selective Ca^{2+} ionophore ionomycin, which raises intracellular Ca^{2+} levels, was added to check cell viability. Representative graphs (left panels) and Ca^{2+} traces (right panels) summarizing Ca^{2+} release (A–D) or uptake (E) are shown. n = 3–7 with a minimum of 16 cells analyzed per experiment (A), n = 3–5 with a minimum of 8 cells analyzed per experiment (B), n = 3–8 with a minimum of 13 cells analyzed per experiment (C), n = 3–7 with a minimum of 14 cells analyzed per experiment (D), and n = 3–4 with a minimum of 16 cells analyzed per experiment (E). Error bars represent the standard error of the mean. *p < 0.05; **p < 0.01; ***p < 0.001. Abbreviations: FU, fluorescence units; s, seconds.

were more susceptible to oxidative stress in response to treatment with the glutathione synthesis inhibitor L-buthionine-(*S*,*R*)-sulfoximine (BSO) at a concentration of 50 μM and increasing concentrations of iron (Fe^{3+} citrate) to increase their oxidative burden (Figure S5A). Treatment with the antioxidant compound EPI-743, which has proven efficacy in rescuing cells from individuals with primary genetic mitochondrial disease,[29] rescued the phenotype of oxidative stress susceptibility with an EC_{50} of 19 nM in these primary dermal fibroblasts, while treatment with a non-redox cycling analog of EPI-743 (RS-743) showed no rescue from oxidative stress challenge when tested at concentrations up to 1,000 nM (Figure S5B). However, oxidative stress susceptibility was not increased in fibroblasts from probands 3 and 4, and proband 1 fibroblasts stably overexpressing wild-type *CCDC47* failed to rescue the molecular phenotype (data not shown). These findings suggest that CCDC47 deficiency does not uniformly lead to increased susceptibility to oxidative stress.

Through detailed clinical phenotyping, whole-exome sequencing analysis, and multicenter collaboration,[18] we identified four unrelated individuals with bi-allelic loss-of-function variants in *CCDC47* who are affected by a multisystem disorder characterized by woolly hair, liver dysfunction, pruritus, dysmorphic features, hypotonia, and global developmental delay (Figures 1, 2A, and 2B, and Table 1). The *CCDC47* variants identified in these four individuals are predicted to truncate CCDC47 (Figure 2C). Analyses of *CCDC47* mRNA and CCDC47 protein in cell lines derived from all four individuals demonstrated that both of these products were severely decreased or absent, supporting the prediction that these variants lead to nonsense-mediated decay and the consequent absence of the protein (Figures 2D–2F and Table 2). Further, we have demonstrated that Ca^{2+} storage, signaling, and refilling are impaired in primary dermal fibroblasts from individuals with bi-allelic loss-of-function variants in *CCDC47* (Figure 3), likely due to reduced levels of the ER Ca^{2+}-binding protein CCDC47. While additional candidate variants were detected in each of the probands (Table S4), *CCDC47* was the only candidate gene common to all four probands.

Of note, we observed some variability in the clinical presentation of the four probands reported in this study. First, proband 1 exhibited severe pancreatitis while the other individuals did not (Table 1). Her unique clinical presentation may be secondary to her gallbladder disease or her genetic background. Second, probands 2 and 3 presented with immunodeficiency and recurrent infections (Table 1). Given

that primary immunodeficiencies have been associated with variants in *STIM1* and *ORAI1* that encode key proteins involved in SOCE,[9,11] immunodeficiency may be a *bona fide* clinical feature of this disorder. Third, probands 3 and 4 exhibited several behavioral issues that the other two probands did not exhibit (Table 1); these behavioral issues might be due to a common change at another genetic locus, although no additional shared rare variants were identified through whole-exome sequencing of these probands. Fourth, proband 4 appears less severely affected compared to the three other probands. For instance, she was able to sit up and she did not have arthrogryposis or hypertelorism (Figure 1D and Table 1). Interestingly, proband 4 had the least severe SOCE molecular defect (Figure 3E). It is possible that there are genetic, environmental, and/or stochastic factors that lead to a variable clinical presentation among these four individuals. The identification and characterization of additional individuals will further help distill the key clinical features of this multisystem disorder that exhibits variable expressivity.

Notably, some of the rare *CCDC47* variants that we detected may be considered founder variants. Proband 2 is of Turkish ancestry with consanguineous parents and homozygous for a rare variant (c.811C>T [p.Arg271*]), whereas probands 3 and 4 are of Amish ancestry and, while unrelated, they both share homozygosis for the same rare variant (c.1145delT [p.Leu382Argfs*2]). These variants may be founder variants in the corresponding populations and, although maintained at very low frequencies, they are more likely to come together in homozygosis due to autozygosity by consanguinity, i.e., identity-by-descent or genetic drift in these populations. Indeed, the homozygous variant c.811C>T in proband 2 was located within a 1.3 Mb region of absence of heterozygosity (AOH) of a total of 268.4 Mb of autozygous genome, evidence of the reported consanguinity in this family (Table 2 and Figure S6A). AOH analyses of probands 3 and 4, both of Amish ancestry, revealed that the shared c.1145delT variant occurs within a 14.11 Mb shared haplotype within larger regions of AOH spanning 19.6 Mb and 15.7 Mb, respectively, in the genomes of these probands (Table 2 and Figure S6B). Therefore, these alleles can be readily included in population-specific disease panels for accurate and rapid molecular diagnosis and carrier or prenatal screening as reported for other founder alleles.[30]

The *Ccdc47*-knockout mouse model provides support for some of the clinical features we observed in our four unrelated individuals.[13,14] Similar to the *Ccdc47*-knockout mouse model, all of the individuals described in this study had decreased body weight and/or poor growth and neurological abnormalities including enlargement of the ventricles and/or cerebral atrophy; some of the individuals had heart abnormalities including PDA and/or VSD. Multiple miscarriages are a notable feature of all four families (Figure 2A). Interestingly, the *Ccdc47*-knockout mouse model generated on a mixed C57BL/6 × 129/Sv genetic background showed variable lethality ranging from embryonic to neonatal lethality.[13] Subsequent backcrossing of this line for more than six generations showed embryonic lethality at midgestation (E10.5–E11.5).[14] It is possible that some of the miscarried fetuses could also harbor bi-allelic variants in *CCDC47*. These observations suggest that there may be genetic modifiers of this clinical phenotype consistent with the variable expressivity observed in individuals with pathogenic *CCDC47* variants.

Ca^{2+} depletion of the ER can lead to ER stress and activation of the UPR pathways.[12] Despite Ca^{2+} depletion in the ER, we observed that the primary dermal fibroblasts derived from proband 1 were still capable of activating all three pathways of the UPR, including the IRE1α, ATF6, and PERK pathways, upon ER stress with thapsigargin similar to that of an unaffected control (Figure S4). Analogous findings have been observed in the *Ccdc47*-knockout MEFs.[13] Interestingly, activation of the IRE1α pathway and increased levels of the ER chaperone protein glucose-regulated protein 78 (GRP78), which is a key regulator of ER stress, an activator of UPR signaling, and a downstream target of UPR,[31,32] have been observed in *CCDC47*-knockdown HEK293 cells without treatment with thapsigargin.[14] These findings may be due in part to differences in cell type and/or due to an acute decrease in *CCDC47* levels.

Susceptibility to oxidative stress was increased in the primary dermal fibroblasts of proband 1, similar to what has been observed in individuals with primary mitochondrial disorders that affect cellular oxidation/reduction processes (Figure S5A). We postulated that the increased susceptibility to oxidative stress may be a secondary downstream effect of CCDC47 deficiency since Ca^{2+} signaling is integral for mitochondrial function and there is extensive crosstalk between the Ca^{2+} and ROS signaling systems.[27,28] However, we observed that fibroblasts from probands 3 and 4 did not show increased susceptibility to oxidative stress and fibroblasts from proband 1 stably overexpressing wild-type *CCDC47* were equally susceptible to oxidative stress as the fibroblasts from proband 1 lacking CCDC47. These findings strongly suggest that CCDC47 deficiency does not increase susceptibility to oxidative stress and that one or more variants, unique to proband 1, contribute to our observations.

Though most of the Ca^{2+} dysregulation disorders are myopathies, unsurprisingly due to the heavy Ca^{2+} dependency of muscle for contraction, we observed a broader and pleiotropic phenotype affecting multiple organs and systems beyond musculoskeletal findings in the case of CCDC47 deficiency. One explanation for the multisystem involvement is that a broader range of cell types and/or developmental stages, in addition to those involved in muscle contraction and development, may be sensitive to *CCDC47* deficiency. Since muscle contraction and synaptic vesicle exocytosis are regulated by Ca^{2+} signaling, it is possible that dysregulation of Ca^{2+} signaling due to CCDC47 deficiency could contribute to the hypotonia and global development delay in our probands. Gastrointestinal complications, including the cholestatic liver disease in probands 3 and 4, exocrine pancreatic insufficiency

in proband 1, and poor growth common to all four probands, are prominent clinical features (Table 1). Ca^{2+} signaling contributes to the regulation of secretion in many cell types, including hepatocytes and cholangiocytes that secrete bile, pancreatic acinar cells that secrete digestive enzymes, and salivary gland acinar cells that secrete saliva.[33–35] All three IP_3R isoforms are the primary Ca^{2+} release channels in the secretory cells of the bile duct, and the loss of IP_3R and subsequent loss of Ca^{2+} release has been shown to contribute to the pathogenesis of cholestatic liver disease.[36,37] Furthermore, mice in which type 2 and type 3 IP_3Rs are absent displayed secretion deficits in the pancreatic and salivary gland acinar cells due to impaired Ca^{2+} signaling that ultimately led to difficulties in nutrient digestion and poor growth.[38] Similarly, all of the individuals in this study presented with poor growth and most were fed by G-tube (Figure 1 and Table 1). Further studies performed in a clinically relevant cell type via *CCDC47*-knockdown cultured cells or in a conditional *Ccdc47*-knockout mouse model are required to delineate the molecular mechanism by which CCDC47 deficiency contributes to these clinical features.

Although we identified impaired Ca^{2+} homeostasis and signaling in primary dermal fibroblasts from individuals with bi-allelic loss-of-function variants in *CCDC47*, there are several other known proteins that have Ca^{2+} buffering capacity in the ER. Examples include calreticulin, heat shock protein 90 beta family member 1 (also known as endoplasmin or GRP94), calnexin, and prolyl 4-hydroxylase subunit beta (also known as protein disulfide isomerase).[39,40] Similar to CCDC47, these proteins bind Ca^{2+} with low affinity and high capacity.[13,41–47] In fact, calreticulin has been shown to bind approximately 50% of the total Ca^{2+} within the ER.[48] Many of these ER Ca^{2+} buffering proteins are multifunctional and, indeed, loss-of-function mouse models generated for several of these showed embryonic lethality,[49–51] which suggests that these proteins have non-overlapping functions. Therefore, it is probable that CCDC47 has yet unexplored and unique roles, aside from its ER Ca^{2+} buffering capacity, that cannot be compensated for by the presence of other Ca^{2+} buffering proteins in the ER. Indeed, CCDC47 has been suggested to regulate Ca^{2+} release-activated Ca^{2+} (CRAC) channels that are responsible for ER filling and interacts with STIM1 and ORAI1 that are responsible for SOCE.[52] Our molecular findings of decreased ER Ca^{2+} and SOCE align with those observed in the *Ccdc47*-knockout MEFs,[13] which suggests that CCDC47 may be involved in regulating SOCE.

In summary, we report that bi-allelic loss-of-function variants in *CCDC47* cause a rare autosomal-recessive disorder characterized by woolly hair, liver dysfunction, pruritus, dysmorphic features, and global developmental delay. Through *in vitro* and cellular experiments, we provide evidence that Ca^{2+} storage and signaling are impaired in primary dermal fibroblasts derived from three individuals with loss-of-function variants in *CCDC47*; however, it is not clear how CCDC47 deficiency leads to the clinical presentation observed in the affected individuals. Additional functional studies will be necessary to better understand the role of CCDC47 in Ca^{2+} homeostasis and signaling in the ER and further elucidate how its absence leads to this developmental disorder.

Accession Numbers

The accession numbers for the variants reported in this paper are ClinVar: SCV000809006, SCV000809007, SCV000809008, and SCV000809009.

Supplemental Data

Supplemental Data include Supplemental Note, Supplemental Subjects and Methods, six figures, and four tables and can be found with this article online at https://doi.org/10.1016/j.ajhg.2018.09.014.

Acknowledgments

We thank all of the individuals presented in the study and their families for their participation in this study. This study was supported in part by the National Human Genome Research Institute (NHGRI) Intramural Research Program; the National Institutes of Health (NIH) Common Fund from the Office of the Director; charitable contributions from Old Order Amish and Mennonite communities of Pennsylvania, Indiana, and surrounding states; the EU Horizon 2020 BATcure consortium grant (666918) to H.W.-E. and E.L.-E.; a research grant from The Royal Society to E.L.-E.; R35 NS105078 to J.R.L.; MDA#512848 to J.R.L.; and a jointly funded NHGRI and National Heart, Lung, and Blood Institute (NHLBI) grant to the Baylor-Hopkins Center for Mendelian Genomics (UM1 HG006542) to J.R.L. E.M. was supported by a PhD studentship from the Niemann-Pick Research Foundation; J.E.P. is supported by NHGRI K08 HG008986.

Declaration of Interests

C.R.H., A.A., and M.K. are employees of BioElectron Technology Corporation, which is developing EPI-743 for the treatment of mitochondrial disease and related disorders. C.G.-J. and J.D.O. are full-time employees of the Regeneron Genetics Center from Regeneron Pharmaceuticals Inc. and receive stock options as part of compensation. J.R.L. has stock ownership in 23andMe and Lasergen, is a paid consultant for Regeneron, and is a co-inventor on multiple United States and European patents related to molecular diagnostics for inherited neuropathies, eye diseases, and bacterial genomic fingerprinting. The other authors declare no conflicts of interest.

Received: June 19, 2018
Accepted: September 26, 2018
Published: October 25, 2018

Web Resources

CADD, https://cadd.gs.washington.edu/
ClinVar, https://www.ncbi.nlm.nih.gov/clinvar/
dbSNP, https://www.ncbi.nlm.nih.gov/projects/SNP/
ExAC Browser, http://exac.broadinstitute.org/

GenBank, https://www.ncbi.nlm.nih.gov/genbank/
gnomAD Browser, http://gnomad.broadinstitute.org/
Human Gene Mutation Database, http://www.hgmd.cf.ac.uk/ac/index.php
OMIM, http://www.omim.org/
PolyPhen-2, http://genetics.bwh.harvard.edu/pph2/
PubMed, http://www.ncbi.nlm.nih.gov/PubMed/
SIFT, http://sift.bii.a-star.edu.sg/

References

1. Berridge, M.J., Bootman, M.D., and Roderick, H.L. (2003). Calcium signalling: dynamics, homeostasis and remodelling. Nat. Rev. Mol. Cell Biol. *4*, 517–529.
2. Somlyo, A.P., Bond, M., and Somlyo, A.V. (1985). Calcium content of mitochondria and endoplasmic reticulum in liver frozen rapidly *in vivo*. Nature *314*, 622–625.
3. Odermatt, A., Taschner, P.E., Khanna, V.K., Busch, H.F., Karpati, G., Jablecki, C.K., Breuning, M.H., and MacLennan, D.H. (1996). Mutations in the gene-encoding SERCA1, the fast-twitch skeletal muscle sarcoplasmic reticulum Ca^{2+} ATPase, are associated with Brody disease. Nat. Genet. *14*, 191–194.
4. Sakuntabhai, A., Ruiz-Perez, V., Carter, S., Jacobsen, N., Burge, S., Monk, S., Smith, M., Munro, C.S., O'Donovan, M., Craddock, N., et al. (1999). Mutations in *ATP2A2*, encoding a Ca^{2+} pump, cause Darier disease. Nat. Genet. *21*, 271–277.
5. Zhang, Y., Chen, H.S., Khanna, V.K., De Leon, S., Phillips, M.S., Schappert, K., Britt, B.A., Browell, A.K., and MacLennan, D.H. (1993). A mutation in the human ryanodine receptor gene associated with central core disease. Nat. Genet. *5*, 46–50.
6. Shen, J., Yu, W.M., Brotto, M., Scherman, J.A., Guo, C., Stoddard, C., Nosek, T.M., Valdivia, H.H., and Qu, C.K. (2009). Deficiency of MIP/MTMR14 phosphatase induces a muscle disorder by disrupting $Ca(^{2+})$ homeostasis. Nat. Cell Biol. *11*, 769–776.
7. Misceo, D., Holmgren, A., Louch, W.E., Holme, P.A., Mizobuchi, M., Morales, R.J., De Paula, A.M., Stray-Pedersen, A., Lyle, R., Dalhus, B., et al. (2014). A dominant *STIM1* mutation causes Stormorken syndrome. Hum. Mutat. *35*, 556–564.
8. Böhm, J., Chevessier, F., Maues De Paula, A., Koch, C., Attarian, S., Feger, C., Hantaï, D., Laforêt, P., Ghorab, K., Vallat, J.M., et al. (2013). Constitutive activation of the calcium sensor STIM1 causes tubular-aggregate myopathy. Am. J. Hum. Genet. *92*, 271–278.
9. Picard, C., McCarl, C.A., Papolos, A., Khalil, S., Lüthy, K., Hivroz, C., LeDeist, F., Rieux-Laucat, F., Rechavi, G., Rao, A., et al. (2009). *STIM1* mutation associated with a syndrome of immunodeficiency and autoimmunity. N. Engl. J. Med. *360*, 1971–1980.
10. Endo, Y., Noguchi, S., Hara, Y., Hayashi, Y.K., Motomura, K., Miyatake, S., Murakami, N., Tanaka, S., Yamashita, S., Kizu, R., et al. (2015). Dominant mutations in ORAI1 cause tubular aggregate myopathy with hypocalcemia via constitutive activation of store-operated Ca^{2+} channels. Hum. Mol. Genet. *24*, 637–648.
11. Feske, S., Gwack, Y., Prakriya, M., Srikanth, S., Puppel, S.H., Tanasa, B., Hogan, P.G., Lewis, R.S., Daly, M., and Rao, A. (2006). A mutation in *Orai1* causes immune deficiency by abrogating CRAC channel function. Nature *441*, 179–185.
12. Mekahli, D., Bultynck, G., Parys, J.B., De Smedt, H., and Missiaen, L. (2011). Endoplasmic-reticulum calcium depletion and disease. Cold Spring Harb. Perspect. Biol. *3*, 3.
13. Zhang, M., Yamazaki, T., Yazawa, M., Treves, S., Nishi, M., Murai, M., Shibata, E., Zorzato, F., and Takeshima, H. (2007). Calumin, a novel Ca^{2+}-binding transmembrane protein on the endoplasmic reticulum. Cell Calcium *42*, 83–90.
14. Yamamoto, S., Yamazaki, T., Komazaki, S., Yamashita, T., Osaki, M., Matsubayashi, M., Kidoya, H., Takakura, N., Yamazaki, D., and Kakizawa, S. (2014). Contribution of calumin to embryogenesis through participation in the endoplasmic reticulum-associated degradation activity. Dev. Biol. *393*, 33–43.
15. Gahl, W.A., and Tifft, C.J. (2011). The NIH Undiagnosed Diseases Program: lessons learned. JAMA *305*, 1904–1905.
16. Gahl, W.A., Markello, T.C., Toro, C., Fajardo, K.F., Sincan, M., Gill, F., Carlson-Donohoe, H., Gropman, A., Pierson, T.M., Golas, G., et al. (2012). The National Institutes of Health Undiagnosed Diseases Program: insights into rare diseases. Genet. Med. *14*, 51–59.
17. Gahl, W.A., Mulvihill, J.J., Toro, C., Markello, T.C., Wise, A.L., Ramoni, R.B., Adams, D.R., Tifft, C.J.; and UDN (2016). The NIH Undiagnosed Diseases Program and Network: Applications to modern medicine. Mol. Genet. Metab. *117*, 393–400.
18. Sobreira, N., Schiettecatte, F., Valle, D., and Hamosh, A. (2015). GeneMatcher: a matching tool for connecting investigators with an interest in the same gene. Hum. Mutat. *36*, 928–930.
19. Richards, S., Aziz, N., Bale, S., Bick, D., Das, S., Gastier-Foster, J., Grody, W.W., Hegde, M., Lyon, E., Spector, E., et al.; ACMG Laboratory Quality Assurance Committee (2015). Standards and guidelines for the interpretation of sequence variants: a joint consensus recommendation of the American College of Medical Genetics and Genomics and the Association for Molecular Pathology. Genet. Med. *17*, 405–424.
20. Thastrup, O., Cullen, P.J., Drøbak, B.K., Hanley, M.R., and Dawson, A.P. (1990). Thapsigargin, a tumor promoter, discharges intracellular Ca^{2+} stores by specific inhibition of the endoplasmic reticulum $Ca^{2(+)}$-ATPase. Proc. Natl. Acad. Sci. USA *87*, 2466–2470.
21. Nelson, O., Tu, H., Lei, T., Bentahir, M., de Strooper, B., and Bezprozvanny, I. (2007). Familial Alzheimer disease-linked mutations specifically disrupt Ca^{2+} leak function of presenilin 1. J. Clin. Invest. *117*, 1230–1239.
22. Bultynck, G., Kiviluoto, S., and Methner, A. (2014). Bax inhibitor-1 is likely a pH-sensitive calcium leak channel, not a H^+/Ca^{2+} exchanger. Sci. Signal. *7*, pe22.
23. Harding, H.P., Zhang, Y., and Ron, D. (1999). Protein translation and folding are coupled by an endoplasmic-reticulum-resident kinase. Nature *397*, 271–274.
24. Haze, K., Yoshida, H., Yanagi, H., Yura, T., and Mori, K. (1999). Mammalian transcription factor ATF6 is synthesized as a transmembrane protein and activated by proteolysis in response to endoplasmic reticulum stress. Mol. Biol. Cell *10*, 3787–3799.
25. Yoshida, H., Matsui, T., Yamamoto, A., Okada, T., and Mori, K. (2001). *XBP1* mRNA is induced by ATF6 and spliced by IRE1 in response to ER stress to produce a highly active transcription factor. Cell *107*, 881–891.
26. Calfon, M., Zeng, H., Urano, F., Till, J.H., Hubbard, S.R., Harding, H.P., Clark, S.G., and Ron, D. (2002). IRE1 couples endoplasmic reticulum load to secretory capacity by processing the *XBP-1* mRNA. Nature *415*, 92–96.

27. Rowland, A.A., and Voeltz, G.K. (2012). Endoplasmic reticulum-mitochondria contacts: function of the junction. Nat. Rev. Mol. Cell Biol. *13*, 607–625.
28. Görlach, A., Bertram, K., Hudecova, S., and Krizanova, O. (2015). Calcium and ROS: A mutual interplay. Redox Biol. *6*, 260–271.
29. Shrader, W.D., Amagata, A., Barnes, A., Enns, G.M., Hinman, A., Jankowski, O., Kheifets, V., Komatsuzaki, R., Lee, E., Mollard, P., et al. (2011). α-Tocotrienol quinone modulates oxidative stress response and the biochemistry of aging. Bioorg. Med. Chem. Lett. *21*, 3693–3698.
30. Strauss, K.A., Gonzaga-Jauregui, C., Brigatti, K.W., Williams, K.B., King, A.K., Van Hout, C., Robinson, D.L., Young, M., Praveen, K., Heaps, A.D., et al. (2018). Genomic diagnostics within a medically underserved population: efficacy and implications. Genet. Med. *20*, 31–41.
31. Li, W.W., Alexandre, S., Cao, X., and Lee, A.S. (1993). Transactivation of the grp78 promoter by Ca^{2+} depletion. A comparative analysis with A23187 and the endoplasmic reticulum $Ca(^{2+})$-ATPase inhibitor thapsigargin. J. Biol. Chem. *268*, 12003–12009.
32. Bertolotti, A., Zhang, Y., Hendershot, L.M., Harding, H.P., and Ron, D. (2000). Dynamic interaction of BiP and ER stress transducers in the unfolded-protein response. Nat. Cell Biol. *2*, 326–332.
33. Petersen, O.H. (2014). Calcium signalling and secretory epithelia. Cell Calcium *55*, 282–289.
34. Ambudkar, I.S. (2014). Ca^{2+} signaling and regulation of fluid secretion in salivary gland acinar cells. Cell Calcium *55*, 297–305.
35. Trampert, D.C., and Nathanson, M.H. (2018). Regulation of bile secretion by calcium signaling in health and disease. Biochim Biophys Acta Mol. Cell. Res. *11*, 1761–1770.
36. Shibao, K., Hirata, K., Robert, M.E., and Nathanson, M.H. (2003). Loss of inositol 1,4,5-trisphosphate receptors from bile duct epithelia is a common event in cholestasis. Gastroenterology *125*, 1175–1187.
37. Martin, J., and Dufour, J.F. (2004). Cholestasis shuts down calcium signaling in cholangiocytes. Hepatology *39*, 248–249.
38. Futatsugi, A., Nakamura, T., Yamada, M.K., Ebisui, E., Nakamura, K., Uchida, K., Kitaguchi, T., Takahashi-Iwanaga, H., Noda, T., Aruga, J., and Mikoshiba, K. (2005). IP_3 receptor types 2 and 3 mediate exocrine secretion underlying energy metabolism. Science *309*, 2232–2234.
39. Michalak, M., Robert Parker, J.M., and Opas, M. (2002). Ca^{2+} signaling and calcium binding chaperones of the endoplasmic reticulum. Cell Calcium *32*, 269–278.
40. Milner, R.E., Famulski, K.S., and Michalak, M. (1992). Calcium binding proteins in the sarcoplasmic/endoplasmic reticulum of muscle and nonmuscle cells. Mol. Cell. Biochem. *112*, 1–13.
41. Baksh, S., and Michalak, M. (1991). Expression of calreticulin in *Escherichia coli* and identification of its Ca^{2+} binding domains. J. Biol. Chem. *266*, 21458–21465.
42. Koch, G., Smith, M., Macer, D., Webster, P., and Mortara, R. (1986). Endoplasmic reticulum contains a common, abundant calcium-binding glycoprotein, endoplasmin. J. Cell Sci. *86*, 217–232.
43. Van, P.N., Peter, F., and Söling, H.D. (1989). Four intracisternal calcium-binding glycoproteins from rat liver microsomes with high affinity for calcium. No indication for calsequestrin-like proteins in inositol 1,4,5-trisphosphate-sensitive calcium sequestering rat liver vesicles. J. Biol. Chem. *264*, 17494–17501.
44. Gilchrist, J.S., and Pierce, G.N. (1993). Identification and purification of a calcium-binding protein in hepatic nuclear membranes. J. Biol. Chem. *268*, 4291–4299.
45. Wada, I., Rindress, D., Cameron, P.H., Ou, W.J., Doherty, J.J., 2nd, Louvard, D., Bell, A.W., Dignard, D., Thomas, D.Y., and Bergeron, J.J. (1991). SSR alpha and associated calnexin are major calcium binding proteins of the endoplasmic reticulum membrane. J. Biol. Chem. *266*, 19599–19610.
46. Tjoelker, L.W., Seyfried, C.E., Eddy, R.L., Jr., Byers, M.G., Shows, T.B., Calderon, J., Schreiber, R.B., and Gray, P.W. (1994). Human, mouse, and rat calnexin cDNA cloning: identification of potential calcium binding motifs and gene localization to human chromosome 5. Biochemistry *33*, 3229–3236.
47. Lebeche, D., Lucero, H.A., and Kaminer, B. (1994). Calcium binding properties of rabbit liver protein disulfide isomerase. Biochem. Biophys. Res. Commun. *202*, 556–561.
48. Nakamura, K., Zuppini, A., Arnaudeau, S., Lynch, J., Ahsan, I., Krause, R., Papp, S., De Smedt, H., Parys, J.B., Muller-Esterl, W., et al. (2001). Functional specialization of calreticulin domains. J. Cell Biol. *154*, 961–972.
49. Mesaeli, N., Nakamura, K., Zvaritch, E., Dickie, P., Dziak, E., Krause, K.H., Opas, M., MacLennan, D.H., and Michalak, M. (1999). Calreticulin is essential for cardiac development. J. Cell Biol. *144*, 857–868.
50. Wanderling, S., Simen, B.B., Ostrovsky, O., Ahmed, N.T., Vogen, S.M., Gidalevitz, T., and Argon, Y. (2007). GRP94 is essential for mesoderm induction and muscle development because it regulates insulin-like growth factor secretion. Mol. Biol. Cell *18*, 3764–3775.
51. Kraus, A., Groenendyk, J., Bedard, K., Baldwin, T.A., Krause, K.H., Dubois-Dauphin, M., Dyck, J., Rosenbaum, E.E., Korngut, L., Colley, N.J., et al. (2010). Calnexin deficiency leads to dysmyelination. J. Biol. Chem. *285*, 18928–18938.
52. Konno, M., Shirakawa, H., Miyake, T., Sakimoto, S., Nakagawa, T., and Kaneko, S. (2012). Calumin, a Ca^{2+}-binding protein on the endoplasmic reticulum, alters the ion permeability of Ca^{2+} release-activated Ca^{2+} (CRAC) channels. Biochem. Biophys. Res. Commun. *417*, 784–789.